JOURNAL OF VIROLOGY, Aug. 2001, p. 7555–7563 Vol. 75, No. 16
0022-538X/01/$04.00+0 DOI: 10.1128/JVI.75.16.7555–7563.2001

Human Parvovirus B19 Induces Cell Cycle Arrest at G_2 Phase with Accumulation of Mitotic Cyclins

EIJI MORITA,[1] KOTARO TADA,[1] HIROSHI CHISAKA,[2] HIRONOBU ASAO,[1] HIROYUKI SATO,[3] NOBUO YAEGASHI,[2] AND KAZUO SUGAMURA[1,4]*

Department of Microbiology and Immunology[1] and Department of Obstetrics and Gynecology,[2] Tohoku University Graduate School of Medicine, and CREST Program of the Japan Science and Technology Corporation,[4] Sendai 980-8575, and Fukuoka Red Cross Blood Center, Fukuoka 818-8588,[3] Japan

Received 26 March 2001/Accepted 23 May 2001

Human parvovirus B19 infects specifically erythroid progenitor cells, which causes transient aplastic crises and hemolytic anemias. Here, we demonstrate that erythroblastoid UT7/Epo cells infected with B19 virus fall into growth arrest with 4N DNA, indicating G_2/M arrest. These B19 virus-infected cells displayed accumulation of cyclin A, cyclin B1, and phosphorylated cdc2 and were accompanied by an up-regulation in the kinase activity of the cdc2-cyclin B1 complex, similar to that in cells treated with the mitotic inhibitor. However, degradation of nuclear lamina and phosphorylation of histone H3 and H1 were not seen in B19 virus-infected cells, indicating that the infected cells do not enter the M phase. Accumulation of cyclin B1 was persistently localized in the cytoplasm, but not in the nucleus, suggesting that B19 virus infection of erythroid cells raises suppression of nuclear import of cyclin B1, resulting in cell cycle arrest at the G_2 phase. The B19 virus-induced G_2/M arrest may be the critical event in the damage of erythroid progenitor cells seen in patients with B19 virus infection.

Human parvovirus B19 is the only pathogenic member of the *Parvoviridae* and causes several diseases in humans, such as transient aplastic crises associated with hemolytic anemias, a common childhood exanthem-erythema infectiosum, some cases of nonimmune hydrops fetalis (NIHF), and chronic bone marrow failure occurring in subjects with immunodeficiency, including AIDS patients (2, 27). B19 virus is a small single-stranded DNA virus that lacks an envelope and specifically infects erythroid progenitor cells (12–14). It has three major proteins: the VP1 and VP2 viral capsid proteins, of which VP2 is a truncated form of VP1; and NS1, a nonstructural protein detected before expression of the VPs and involved in regulation of viral genome replication and gene expression (2, 9, 22). B19 virus infection induces apoptosis and cell cycle arrest at G_2/M phase in primary erythroid progenitor cells as well as erythroid cell lines (22). B19 virus-induced apoptosis and cell cycle arrest have been shown to be mediated by NS1 (9, 22). However, the mechanisms of NS1-mediated apoptosis and cell cycle arrest are still unknown.

The cell cycle progression is critically regulated by sequential activation of cyclin-dependent kinases (cdks). The activities and specificities of cdks are determined by phosphorylation of their catalytic subunits and by their associations with various inhibitors and cyclins, which are differentially expressed during the cell cycle (10, 16). Cyclins A and B are involved in regulation of the S and G_2/M phases of the cell cycle (10, 16). Expression of cyclin A becomes detectable near the G_1/S transition, peaks in the S phase, and interacts with both cdk2 and cdc2 to ensure completion of DNA replication before entering into mitosis (8). Cyclin B is synthesized through the S and G_2 phases and associates with cdc2 to become an inactive complex, called the pre-mitosis-promoting factor (pre-MPF). In the subsequent G_2/M transition, cdc2 in the pre-MPF is dephosphorylated by cdc25C-specific phosphatase, resulting in conversion from the pre-MPF to an active MPF complex in the cytoplasm (8, 10). The activated MPF is then imported into the nuclei to promote the onset of mitosis. MPF inactivation occurs during anaphase by degradation of cyclin B through the ubiquitin pathway, allowing cells to exit from mitosis and cell division (15).

We recently established a cell line, UT7/Epo-S1, highly susceptible to B19 virus infection. UT7/Epo-S1 is a subline derived from UT7/Epo, which is an erythropoietin (Epo)-dependent cell line, and originating from UT7, a megakaryocytic leukemia cell line (21). We demonstrate here that human parvovirus B19 induces cell cycle arrest at G_2 phase in B19 virus-infected UT7/Epo-S1 cells, in which nuclear import of cyclin B1 is significantly impaired.

MATERIALS AND METHODS

Cells. Various clones of UT7/Epo cells (21) were screened for susceptibility to B19 virus infection, and a clone named UT7/Epo-S1 was established as the most susceptible clone. UT7/Epo-S1 cells were propagated in RPMI 1640 medium containing 10% fetal calf serum (FCS) and 2 U of recombinant Epo per ml (a gift from Kirin Brewery Pharmaceutical Research Laboratory, Tokyo, Japan).

Virus infection and neutralization. B19 virus antigen-positive human serum obtained from a blood donor was used as a B19 virus seed, the virus titer of which was calculated to be 10^8 infectious units per milliliter by anti-VP1/2 immunostaining assays. UT7/Epo-S1 cells were inoculated with a multiplicity of infection of 10 with 20-fold-diluted virus seed at 10^6 cells/ml in Iscove's modified Dulbecco's medium (IMDM) and incubated for 2 h at 4°C for virus adsorption. The cells were then diluted to 2×10^5 cells/ml in IMDM containing 10% FCS and 2 U of Epo per ml and cultured at 37°C and 2% CO_2 in air. For B19 virus neutralization assays, the B19 virus seed was preincubated with anti-B19 virus-positive or anti-B19 virus-negative human serum for 60 min at 37°C and then used for infection of UT7/Epo-S1 cells.

TUNEL staining. Terminal deoxynucleotidyltransferase-mediated dUTP-biotin nick end labeling (TUNEL) assays were performed as described elsewhere (24). In brief, cells were dried, fixed in 4% paraformaldehyde (PFA)–phosphate-

* Corresponding author. Mailing address: Department of Microbiology and Immunology, Tohoku University School of Medicine, 21-Seiryo-machi, Aoba-ku, Sendai 980-9575, Japan. Phone: 81-22-717-8096. Fax: 81-22-717-8097. E-mail: sugamura@mail.cc.tohoku.ac.jp.

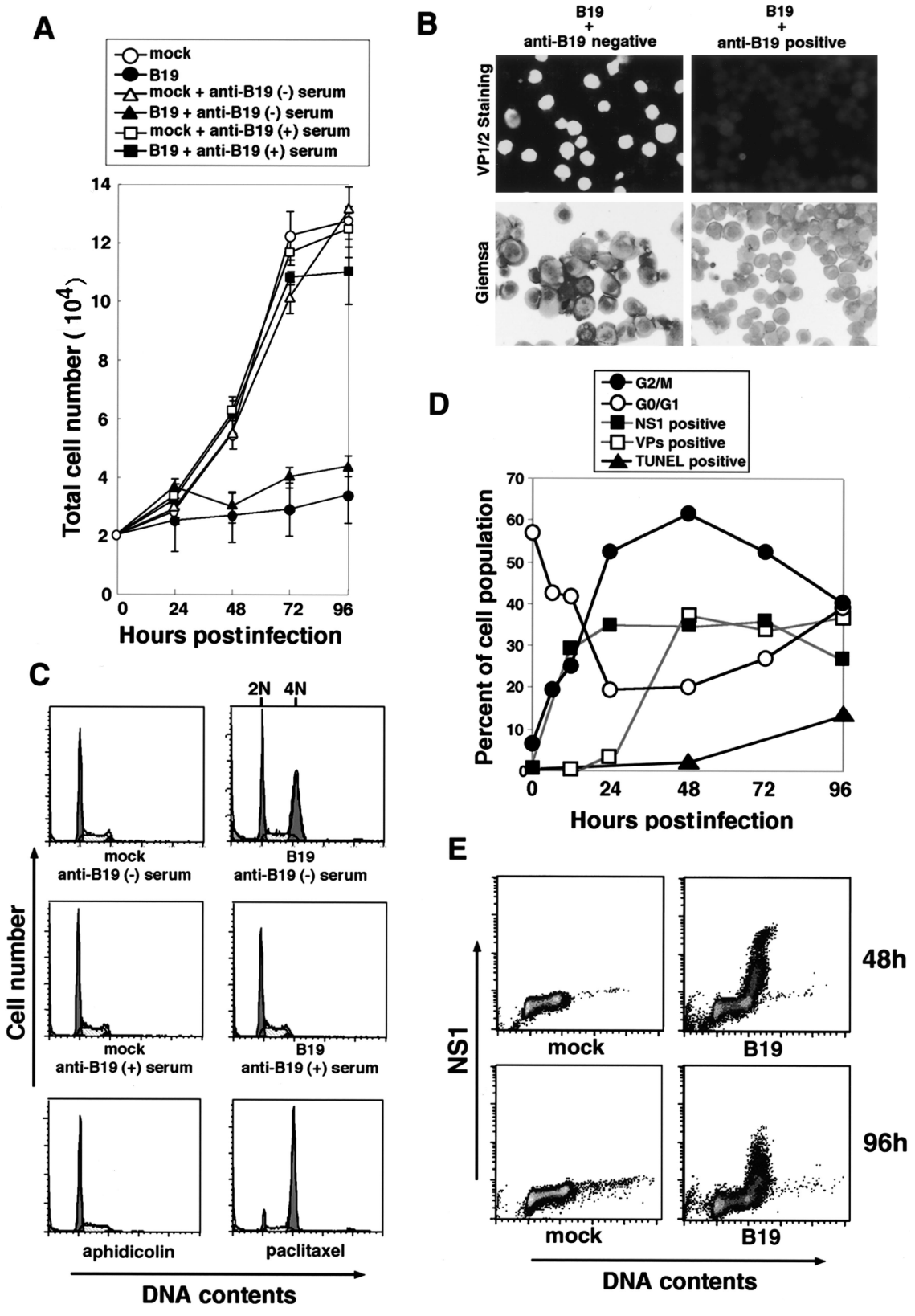

FIG. 1. B19 virus infection leads the cell growth arrest at the G_2/M phase. (A) Growth curves of B19 virus-infected and mock-infected UT7/Epo-S1 cells. UT7/Epo-S1 cells were infected with B19 virus and untreated (●) or pretreated with anti-B19 virus-negative (▲) and -positive (■) serum, or were mock untreated (○) or pretreated with anti-B19 virus-negative (△) and -positive (▲) serum. (B) Immunostaining for B19 virus VP1/2 and Giemsa staining of B19 virus-infected cells. UT7/Epo-S1 cells were infected with B19 virus pretreated with anti-B19 virus-negative

buffered saline (PBS) for 15 min, and then used for terminal transferase labeling of fragmented DNA with a TACS 2 TdT-Blue Label kit (TREVIGEN Inc.) according to the kit's assay protocol.

Cell cycle analysis. Cell cycle analyses were performed as described previously (3). In brief, after the cells had been washed twice with PBS, they were suspended in propidium iodide (PI) solution (50 μg of PI per ml, 0.1% sodium citrate, 0.2% NP-40, 0.25 mg of RNase per ml) and then incubated for 30 min at 4°C. PI-positive cells were counted with a FACScan fluorescence-activated cell sorter (FACS).

Western blotting. Western blot analyses were carried out as described elsewhere (1). In brief, cells were lysed in an aliquot volume of whole-cell extraction buffer (10 mM $NaHPO_4$, 1 mM EDTA, 1 mM dithiothreitol [DTT], 400 mM KCl, 10% glycerol, 5 μg of aprotinin per ml, 10 μg of leupeptin per ml, 2 μM pepstatin, 1 mM phenylmethylsulfonyl fluoride, 5 mM NaF, 1 mM $Na3VO_4$). After freeze and thaw cycles, cell lysates were then microcentrifuged at 28,000 × *g* for 20 min to remove cell debris. After 10 μg of protein from supernatant was separated by sodium dodecyl sulfate-polyacrylamide gel electrophoresis (SDS-PAGE) with 10 to 12% polyacrylamide, proteins were transferred to nitrocellulose membrane (Millipore) by electroblotting for 1.5 h at 40 V in an ATTO semidry blotting system. The membrane was then incubated for 1 h in blocking buffer (Tris-buffered saline [TBS] solution containing 1% Tween 20 and 5% bovine serum albumin) and further incubated for 3 h at room temperature with the following antibodies: a newly established mouse monoclonal antibody (MAb) (immunoglobulin G1 [IgG1]), ParC-NS1, specific for the NS1 C-terminal half of B19 virus, rabbit anti-phospho-cdc2 (Tyr15) (Cell Signaling), mouse anti-cdc2 antibody (17) (Santa Cruz Biotechnology, Santa Cruz, Calif.), mouse anti-cyclin B1 (Upstate Biotechnology Inc.), rabbit anti-cyclin A (C-19) (Santa Cruz), mouse anti-cyclin D1 (Upstate Biotechnology), mouse anti-cyclin D3 (Upstate Biotechnology), rabbit anti-phospho H3 (Upstate Biotechnology), rabbit anti-phospho H1 (Upstate Biotechnology), goat anti-histone H3 (N-20) (Santa Cruz), and mouse anti-histone H1 (Santa Cruz). Bound antibodies were then reacted with horseradish peroxidase-conjugated antimouse, antirabbit, or antigoat antibodies, respectively, and then washed extensively and revealed with a sensitive enhanced chemiluminescence detection system (ECL detection kit; Amersham).

Histone H1 kinase assay. The extracts were prepared by resuspending cells in ice-cold lysis buffer (50 mM HEPES [pH 7.0], 250 mM NaCl, 0.1% NP-40, 10% glycerol, 1 mM DTT, 1 mM phenylmethylsulfonyl fluoride, 5 μg of pepstatin per ml, 2 μg of aprotinin per ml). Lysates containing equal quantities of proteins were incubated with either MAb specific for cyclin B1 (Upstate Biotechnology) or a polyclonal antibody raised against the C terminus of cdc2 (Babco). Immune complexes were isolated with protein A-conjugated Sepharose (Pharmacia). Sepharose pellets were washed with lysis buffer and incubated for 30 min at 37°C in 10 μl of reaction buffer (20 mM HEPES [pH 7.9], 5 mM $MgCl_2$, 1 μg of histone H1 (Wako), 1 mM DTT, 100 μM unlabeled ATP, and 10 μCi of [γ-^{32}P]ATP. The reaction was stopped by the addition of SDS sample buffer and boiled for 5 min, and fractionation was performed by SDS-PAGE on 12% polyacrylamide gels. Gels were dried prior to autoradiography.

RPA. Total RNA from UT7/Epo-S1 cells was prepared after 48 and 96 h of B19 virus infection or 24 h after aphidicolin treatment (10 ng/ml) (Waco), and hybridized to RNA probes of human cyclins by using a Multiprobe RNase protection assay (RPA) system (Riboquant; Pharmingen, San Diego, Calif.) according to the manufacturer's instructions. Briefly, 10 μg of the total RNA was hybridized to a ^{32}P-labeled hCYC1 template set (6×10^5 cpm per sample) for 16 h at 56°C and then subjected to RNase A plus T1 digestion, proteinase K digestion, phenol-chloroform extraction, and ethanol precipitation. The samples were separated by electrophoresis on a 5% acrylamide–bisacrylamide (29:1) urea-containing gel and autoradiographed.

Immunocytochemistry. Cells were fixed in 4% paraformaldehyde (PFA)–PBS for 15 min and stained with the following antibodies: anti-NS1 MAb (ParC-NS1), anti-VP1/2 MAb (Par3) (28), anti-phospho H3 rabbit polyclonal antibody (Upstate Biotechnology), anti-lamin B goat polyclonal antibody (M-20) (Santa Cruz), and anti-cyclin B1 rabbit polyclonal antibody (H-422) (Santa Cruz). They were secondarily stained with fluorescein isothiocyanate (FITC)-conjugated antimouse IgG antibody and either rhodamine-conjugated antirabbit IgG antibody or anti-goat IgG antibody.

RESULTS

B19 virus induces cell cycle arrest and apoptosis. Human parvovirus B19 was first examined for its effect on target cell survival. UT7/Epo-S1 cells were infected with B19 virus, which had been pretreated with anti-B19 virus antibody-positive or -negative human serum, and then cultured in vitro. Their growth curves were plotted with viable cell numbers for 96 h postinfection. The growth of UT7/Epo-S1 cells was almost completely suppressed after B19 virus infection, and this growth arrest was fully abrogated by the pretreatment of B19 virus with anti-B19 virus antibody-positive but not -negative human serum (Fig. 1A). We confirmed that anti-B19 virus antibody-positive human serum completely neutralized the infectivity of B19 virus to UT7/Epo-S1 cells by immunostaining with anti-VP1/2 MAb at 72 h postinfection (Fig. 1B). Furthermore, B19 virus-infected UT7/Epo-S1 cells morphologically demonstrated an enlargement of cell size (Fig. 1B).

The cell cycle analysis based on DNA content detected by FACS was performed with UT7/Epo-S1 cells 72 h after B19 virus infection. The cells were treated with aphidicolin and paclitaxel, which are the S- and M-phase inhibitors, respectively, as controls. Cells containing 2N DNA, which are in the G_0/G_1 phase, were detected in both B19 virus-infected and mock-infected UT7/Epo-S1 cell cultures, while cells containing 4N DNA, which are in the G_2/M phase, were significantly increased only in the B19 virus-infected cell culture, but not in the mock-infected cell culture (Fig. 1C). Pretreatment of B19 virus with anti-B19 virus antibody-positive human serum abrogated the appearance of cells containing 4N DNA (Fig. 1C), suggesting that B19 virus infection induces cell growth arrest at the G_2/M phase.

Cell cycle analysis was sequentially performed after B19 virus infection. The percentage of the G_2/M-phase cell population containing 4N DNA was appreciably increased after B19 virus infection to reach a peak (60%) 48 h after infection and then gradually decreased. The G_0/G_1-phase cell population was decreased after B19 virus infection in a mirror image of the G_2/M-phase cell population (Fig. 1D). B19 virus-infected cells detected by immunofluorescence staining with anti-NS1 MAb were also increased in a pattern similar to that in the G_2/M-phase cells; however, the plateau level of NS1-positive cells was 35% 24 h after infection, which is significantly lower than the peak of the G_2/M-phase cell population (Fig. 1D). The detection sensitivity for NS1 may be significantly lower than that for the G_2/M-phase cells. VP1/2-positive cells increased after 24 h

serum (left panels) or anti-B19 virus-positive serum (right panels). They were immunostained with anti-VP1/2 MAb (Par3) and FITC-conjugated anti-mouse IgG secondary antibody or stained with Mey-Giemsa 72 h postinfection. (C) Flow cytometric analyses of UT7/Epo-S1 cells stained with PI. UT7Epo-S1 cells were infected with B19 virus or mock infected; these cells were pretreated with anti-B19-negative (upper panels) or -positive (middle panels) serum. After 72 h of cultivation, they were stained with PI for detection of DNA content and loaded in a FACScaliber FACS. UT7Epo-S1 cells were also treated with aphidicolin or paclitaxel and stained with PI (bottom panels). (D) Sequential analyses of cell cycle arrest, expression of viral proteins, and apoptosis in B19 virus-infected UT7/Epo-S1 cells. Percentages of G_2/M-phase (●), G_0/G_1-phase (○), NS1-positive (■), VP1/2-positive (□), and TUNEL-positive (▲) cell populations were determined by PI staining or immunostainig at the indicated times after B19 virus infection. (E) Intracellular immunostaining of NS1 and PI staining in B19 virus-infected UT7/Epo-S1 cells. B19 virus- or mock-infected UT7/Epo-S1 cells were stained with anti-NS1 MAb and PI 48 and 96 h postinfection.

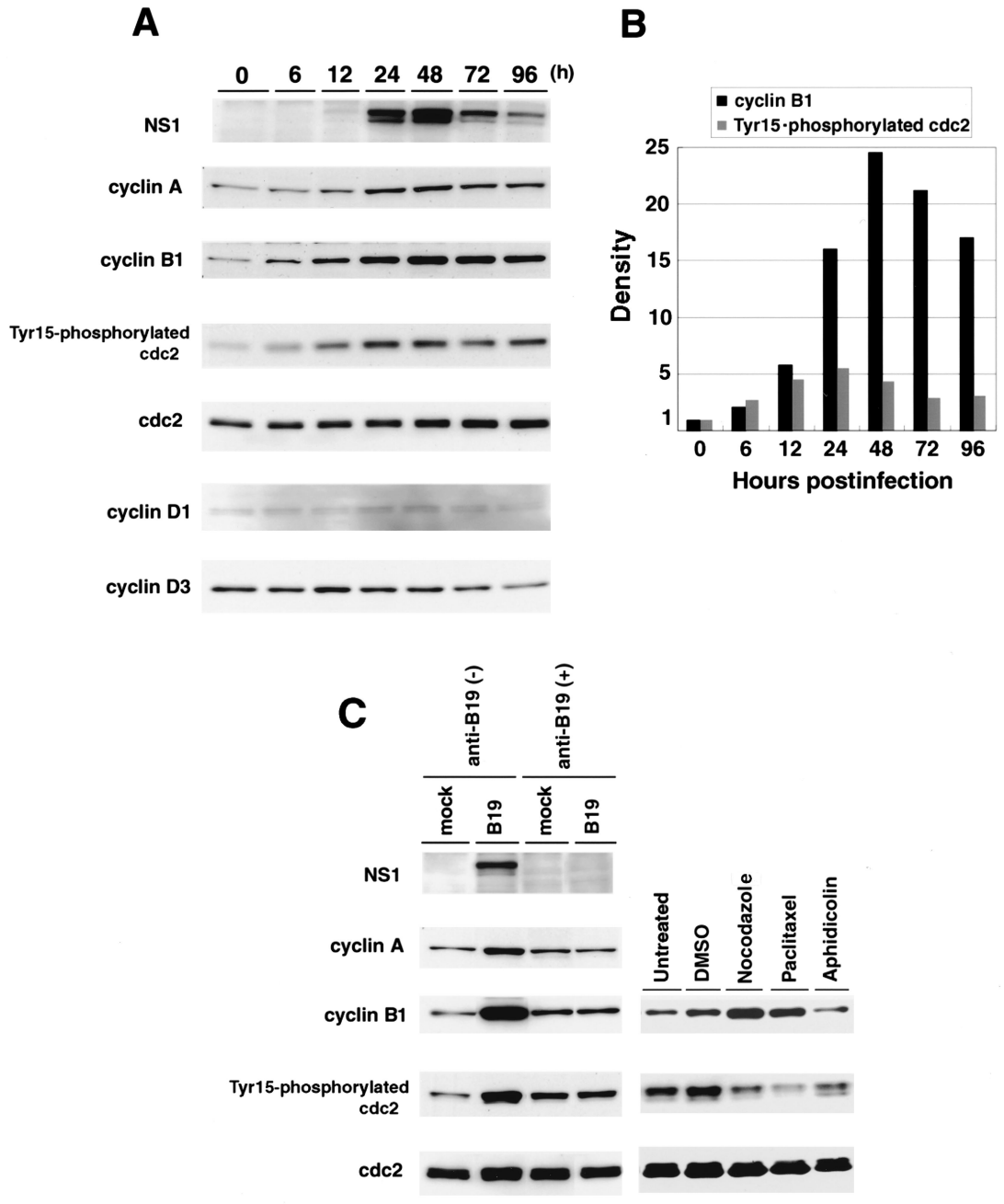

FIG. 2. Accumulation of cyclin A, cyclin B1, and Tyr15-phosphorylated cdc2 in B19 virus-infected cells. (A) Sequential analysis of expression of cell cycle-associated proteins in B19 virus-infected UT7/Epo-S1 cells. UT7/Epo-S1 cells were infected with B19 virus. They were sequentially harvested after infection, and their lysates were separated by SDS-PAGE and transferred to nylon membranes. Western blot analyses were performed with anti-NS1 (ParC-NS1), anti-cyclin B1, anti-cyclin A, anti-phospho-cdc2 (Tyr15), anti-cdc2, anti-cyclin D1, and cyclin D3 antibodies, respectively. Corresponding proteins were detected with enhanced chemiluminescence reagents. (B) Quantification of expression levels of cyclin B1 and Tyr15-phosphorylated cdc2 in B19 virus-infected cells. Immunoblotted bands of cyclin B1 and Tyr15-phosphorylated cdc2 in panel A were measured with a densitometer. Their densities are represented as relative amounts compared with those at 0 h poistinfection. (C) Effects of B19 virus neutralization on accumulation of the cell cycle-associated proteins in B19 virus-infected cells. UT7/Epo-S1 cells were infected with B19 virus or mock infected. These cells were pretreated with anti-B19-positive or -negative serum. They were harvested 48 h postinfection (left panels). UT7/Epo-S1 cells were treated for 24 h with nocodazole, paclitaxel, or aphidicolin suspended in dimethyl sulfoxide (DMSO) (right panels). Their lysates were used for detection of NS1, cyclin A, cyclin B1, Tyr15-phosphorylated cdc2, and total cdc2 by immunoblotting.

of infection, later than the appearance of NS1-positive cells (Fig. 1D). TUNEL-positive cells increased after 48 h of infection, in accordance with a decrease in the G_2/M-phase cells (Fig. 1D). These results suggest the possibility that the G_2/M-phase-arrested cells move into apoptosis. We were unable to detect NS1-positive cells in the G_0/G_1 phase at 48 and 96 h postinfection (Fig. 1E), indicating that all of the cells expressing NS1 arrested at the G_2/M phase.

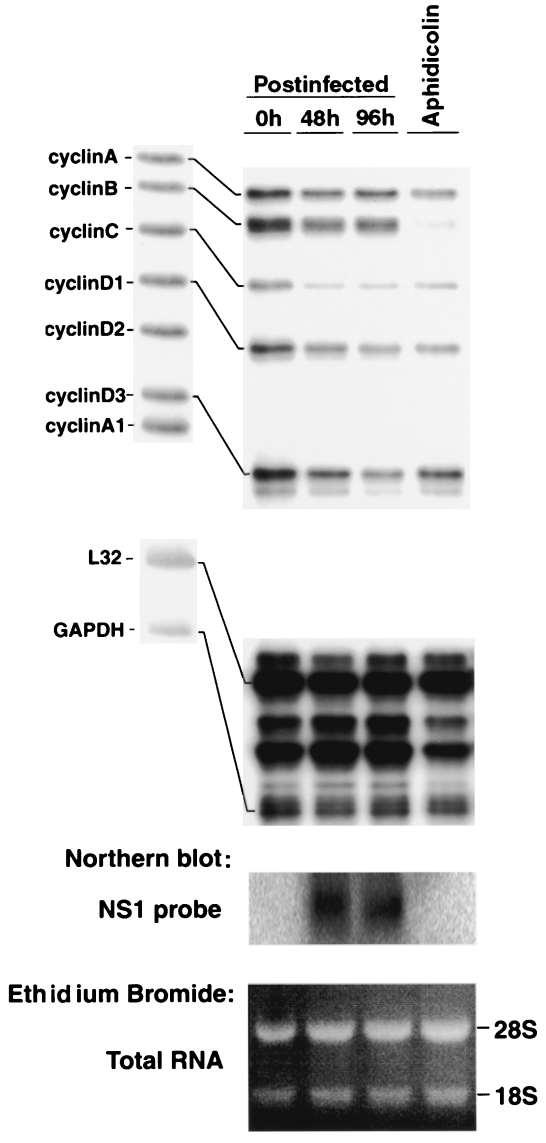

FIG. 3. Gene expression for cyclins in B19 virus-infected UT7/Epo-S1 cells. RPAs were performed with 10 μg of total RNA from cells harvested 0, 48, and 96 h after B19 virus infection or 24 h after aphidicolin treatment, by using the hCYC1 multiprobe. Approximately 500 cpm of ^{32}P-labeled multiprobe was loaded on the left side, and the corresponding RNA species was marked on the right-hand side (upper panel). The RNA species in the probe lane show slightly higher molecular weights than those in other lanes due to the presence of flanking regions in the in vitro transcripts. The surplus RNA samples were used for Northern blotting to check NS1 mRNA expression (middle panel). An equal amount of total RNA in each sample, used for Northern blotting, is shown in the bottom panel. Ethidium bromide staining was performed before membrane transfer. 28S and 18S rRNAs were seen.

Accumulation of cyclin A and B1 and phosphorylated cdc2 in B19 virus-infected cells. To address the molecular mechanism of the B19 virus-induced cell cycle arrest at G_2/M phase, we examined the expression kinetics of cell cycle regulatory molecules such as total cdc2, tyrosine (Tyr15)-phosphorylated cdc2, and cyclin A, B1, D1, and D3 during 96 h after B19 virus infection. In B19 virus-infected UT7/Epo-S1 cells, NS1 expression became detectable at 24 h, reached a peak 48 h postinfection, and then gradually decreased (Fig. 2A). Expression levels of cyclin B1, cyclin A, and Tyr15-phosphorylated cdc2, which are known to be regulators of the cell cycle G_2-M transition (10, 16), were significantly increased after 12 h of infection, reached peaks 24 h or 48 h postinfection, and decreased at 96 h postinfection. However, in spite of an increase in Tyr15-phosphorylated cdc2, the expression level of total cdc2 was unchanged. (Fig. 2A), suggesting that the increased Tyr15-phosphorylated cdc2 may be controlled at the posttranslational level. Furthermore, we quantified the expression levels of cyclin B1 and Tyr15-phosphorylated cdc2 by densitometric analysis; 15- and 25-fold increases in cyclin B1 expression were detected 24 and 48 h postinfection, respectively, while the maximum fivefold increase in Tyr15-phosphorylated cdc2 expression was detected 24 h postinfection (Fig. 2B). These results indicate that the magnitude of cyclin B1 expression is significantly higher than that of Tyr15-phosphorylated cdc2. In contrast, expression levels of cyclin D1 and cyclin D3, which are known to be involved in the cell cycle G_1-S transition (19), were little changed up to 96 h postinfection (Fig. 2A). When B19 virus was pretreated with anti-B19 virus antibody-positive serum before infection of UT7/Epo-S1 cells, the increases in cyclin B1, cyclin A, and Tyr15-phosphorylated cdc2 were not detected (Fig. 2C). As controls, we detected a significant increase in cyclin B1 and a significant decrease in Tyr15-phosphorylated cdc2 in UT7/Epo-S1 cells treated with the mitotic inhibitors nocodazole and paclitaxel (Fig. 2C).

Next, we examined whether the increased expression of mitotic cyclins B1 and A in the B19 virus-infected UT7/Epo-S1 cells was at a transcription level. RPAs were carried out to quantify mRNA expression of cyclins B1, A, D1, and D3 in UT7/Epo-S1 cells after B19 virus infection. The mRNA levels for all four cyclins were slightly decreased after 48 and 96 h of B19 infection, but never increased (Fig. 3). As a control, UT7/Epo-S1 cells treated with aphidicolin showed little expression of cyclin B1 mRNA, and NS1 gene expression was detected 48 and 96 h after infection (Fig. 3). These results suggest that the increase in cyclins A and B1 in the B19 virus-infected cells may be controlled at a posttranscriptional level.

Consecutively, we examined the kinase activity of the cdc2-cyclin B1 complex by using histone H1 as a substrate. B19 virus-infected UT7/Epo-S1 cells were harvested at 72 h postinfection, and as a control, UT7/Epo-S1 cells were treated with an S-phase inhibitor, aphidicolin, or an M-phase inhibitor, nocodazole. Their lysates were immunoprecipitated with anti-cyclin B1 or anti-cdc2 antibody, and the immunoprecipitates were tested for their kinase activities with the histone H1 substrate. Appreciable kinase activities were detected in the immunoprecipitates of the B19 virus-infected cell lysates with either anti-cyclin B1 or anti-cdc2 antibody comparably to those of the nocodazole-treated cell lysates, while the kinase activity was undetectable in those of the aphidicolin-treated cell lysates (Fig. 4). Furthermore, the kinase activities in the B19 virus-infected cell lysates were diminished by pretreatment of B19 virus with anti-B19 antibody-positive serum before infection (Fig. 4). These results indicate that the cdc2-cyclin B1 complex can be activated in the B19 virus-infected cells, suggesting that the activation pathway of the cdc2-cyclin B1 complex is not impaired by B19 virus infection.

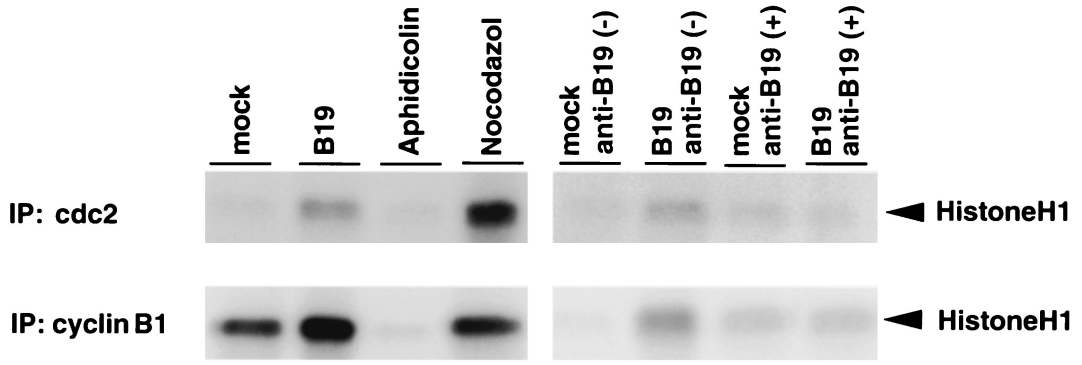

FIG. 4. B19 virus infection up-regulates the kinase activity of the cdc2-cyclin B1 complex. The kinase activity of the cdc2-cyclin B complex was measured as described in Materials and Methods. UT7/Epo-S1 cells were infected with B19 virus or mock infected. These cells were pretreated with anti-B19-positive or -negative serum and harvested 48 h postinfection. UT7/Epo-S1 cells were also treated with aphidicolin and nocodazole and harvested after 24 h of treatment. Aliquots of immunoprecipitated complexes with anti-cdc2 and anti-cyclin B1 antibody, corresponding to 30 and 100 μg of total proteins in the original lysate, respectively, were used for histone H1 kinase activities.

B19 virus-infected cells fall into G_2 arrest, but not mitotic arrest. Mitotic arrest is known to be caused by a deficiency in degradation of either cyclin B1 or cyclin A, which is accompanied by constitutive activation of MPF (8, 15). As described above, in the B19 virus-infected UT7/Epo-S1 cells, these mitotic cyclins were accumulated, and MPF was activated, similar to the cells treated with the mitotic inhibitor nocodazole. Hence, we asked whether the cells infected with B19 virus are able to enter mitosis. For this study, B19 virus-infected UT7/Epo-S1 cells were examined for phosphorylations of histones H1 and H3, known as markers for mitosis (5). UT7/Epo-S1 cells were infected with B19 virus, mock infected, or treated with the mitotic inhibitors nocodazole and paclitaxel. The cells were harvested 48 h after infection or 24 h after drug treatment, and their lysates were examined for phosphorylation of histones H1 and H3 by Western blotting. Unexpectedly, phosphorylated histones H1 and H3 were not detected in the B19 virus-infected cells, whereas phosphorylation of H1 and H3 was up-regulated in the cells treated with the mitotic inhibitors (Fig. 5A). Immunocytochemical examinations of H3 phosphorylation were also performed with B19 virus-infected UT7/Epo-S1 cells. After 72 h of infection, the cells were stained with anti-phospho-H3 antibody together with anti-NS1 MAb. NS1-positive cells were not doubly stained with anti-phospho-H3 antibody (Fig. 5B). To further confirm that NS1-positive cells are negative for phospho-H3, the infected cells were treated with a mitotic inhibitor, paclitaxel, 24 h postinfection. Although phospho-H3-positive cells were signifcantly increased, there were no cells doubly positive for phospho-H3 and NS1 in the paclitaxel-treated B19 virus-infected cells (Fig. 5B). These results suggested that B19 virus-infected cells were unable to enter into mitosis. Although the in vitro histone H1 kinase activity associated with the cdc2-cyclin B1 complex was increased in the B19 virus-infected cells, as shown in Fig. 4, the in vivo phosphorylation of histone H1 was not significantly enhanced in the B19 virus-infected cells. These results indicate that the cdc2-cyclin B1 complex harboring the histone H1 kinase activity is significantly increased in the B19 virus-infected cells because of the accumulation of the cyclin B1. However, the cdc2-cyclin B1 complex is not effective in the phosphorylation of H1 in the B19 virus-infected cells. Furthermore, since nuclear lamina formation is known to be suppressed during mitosis (4), the B19 virus-infected cells were examined for nuclear lamina formation by immunostaining with anti-lamin B antibody 72 h postinfection. The B19 virus-infected cells expressed NS1 in cytoplasm or nucleus, and NS1-positive cells showed nuclear lamina formation around the chromosomes (Fig. 5B); collectively, these results support the conclusion that the B19 virus-infected cells do not enter mitosis.

Since cyclin B1 is known to be localized in the cytoplasm at the G_2 phase and to be transported into the nucleus during the M phase (11, 17, 18, 25, 29, 30), we examined the subcellular localization of cyclin B1 in UT7/Epo-S1 cells after 48 and 96 h of B19 virus infection. The cells were stained with anti-NS1 MAb and anti-cyclin B1 antibody, and positive cells were counted. The percentages of NS-1-positive and cyclin B1-positive and NS1/cyclin B1 double-positive cells were significantly increased after B19 virus infection (Fig. 6A and B). Almost all of the cyclin B1-positive cells included NS1-positive cells. Although NS1 was detectable in both the cytoplasm and nucleus, cells doubly stained for cyclin B1 and NS1 showed a restricted localization of cyclin B1 to only the cytoplasm, but not the nucleus (Fig. 6A). These results suggest the possibility that the nuclear transport of cyclin B1 is inhibited in the B19 virus-infected cells, which further leads to the cell cycle arrest at the G_2 phase.

DISCUSSION

We succeeded here in the establishment of a cell line, UT7/Epo-S1, highly susceptible to human parvovirus B19 infection. More than 40% of UT7/Epo-S1 cells became VP1/2 positive after B19 virus infection, which allowed us to analyze cellular events occurring in the B19 virus-infected cells. B19 virus infection is known to induce apoptosis and G_2/M cell cycle arrest in erythroid progenitor cells, both of which are mediated by NS1 of B19 products (22). The present study revealed that B19 virus-infected UT7/Epo-S1 cells were unable to enter into the mitotic phase and arrested at the G_2 phase.

During the normal cell cycle progression, cyclin B1 accumulates in the S and G_2 phases to form the inactive MPF (pre-MPF) consisting of cyclin B1 and cdc2. Dephosphorylation of

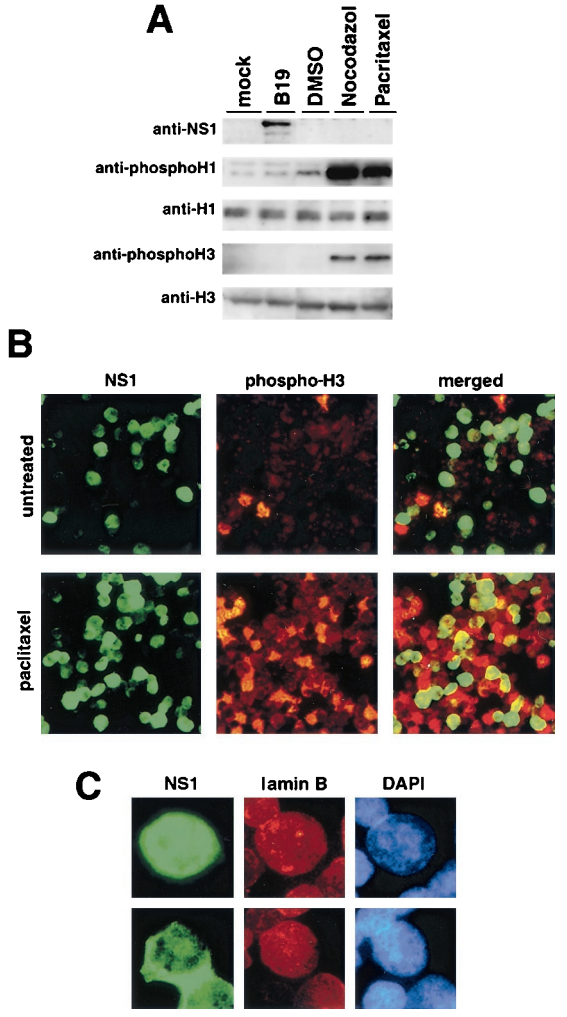

FIG. 5. B19 virus-infected cells do not enter the mitotic stage. (A) Western blot analysis of UT7/Epo-S1 cells infected with B19 virus or mock infected and treated with DMSO, nocodazole, or paclitaxel. Lysates were separated by SDS-PAGE, transferred to nylon membranes, and then incubated with anti-NS1 (ParC-NS1), anti-phospho H1, anti-histone H1, anti-phospho-H3, and anti-histone H3 antibodies, respectively. Corresponding proteins were detected with enhanced chemiluminescence reagents. (B) Immunostaining of B19 virus-infected cells with anti-NS1 MAb and anti-phospho-H3 antibody. At 24 h after infection, B19 virus-infected UT7/Epo-S1 cells were untreated (upper panels) or treated with a mitotic inhibitor, paclitaxel (lower panels), for 24 h. Subsequently, they were stained with anti-NS1 mouse MAb and anti-phospho-H3 rabbit antibody, and then with FITC-conjugated anti-mouse IgG and rhodamine-conjugated anti-rabbit IgG, respectively. The merged images are shown on the right, indicating there were no overlapping cells for NS1 and phospho-H3. (C) Staining of B19 virus-infected cells for NS1, laminin B, and DNA. B19 virus-infected UT7/Epo-S1 cells 48 h after infection were stained with anti-NS1 mouse MAb and anti-laminin B goat antibody and then with FITC-conjugated anti-mouse IgG and rhodamine-conjugated anti-goat IgG, respectively. NS1 was detected in the nucleus (upper panels) and cytoplasm (lower panels). Nuclei were detected by DNA staining with 4′, 6′-diamidino-2-phenylindole.

cdc2 at Tyr15 is required for the MPF activation, and the activated MPF complex translocates from the cytoplasm into the nucleus to initiate mitosis (17, 18, 29). Cyclin B1 in the MPF is then completely degraded at the onset of anaphase by the ubiquitination system (8, 15). However, in the B19 virus-infected UT7/Epo-S1 cells, cyclin B1 accumulated in the cytoplasm, but not in the nucleus, from 24 h postinfection without up-regulation of its mRNA in the cytoplasm. Translocation of active MPF containing cyclin B1 from the cytoplasm into the nucleus is indispensable for cell cycle entry into the M phase (25, 30). We observed that the in vitro histone H1 kinase activity of MPF was significantly enhanced; however, the in vivo phosphorylation of histone H1 was not increased in the B19 virus-infected cells. These observations suggest that activated MPF, present in the cytoplasm, did not translocate to the nucleus, where MPF contributes to phosphorylation of histone H1 (5) and probably H3. Hence, we suspect that B19 virus infection induces inhibition of translocation of MPF from the cytoplasm into the nucleus, which results in suppression of cell cycle transition from the G_2 phase into the M phase. The observation that all of the B19 virus-infected cells have nuclear lamina formation also supports our hypothesis that B19 virus-infected cells do not enter M phase. On the other hand, the MPF activity is known to be negatively regulated by Tyr15 phosphorylation of cdc2 (10, 16). However, although the Tyr15-phosphorylated cdc2 was significantly increased in the B19 virus-infected cells compared to the level in the mock-infected cells, the MPF activity of the B19 virus-infected cells was appreciably higher than that of the mock-infected cells. These discrepant observations can be explained by the fact that the magnitude of cyclin B1 expression is significantly higher than that of Tyr15-phosphorylated cdc2 expression in the B19 virus-infected cells, which results in an increase in both the active and inactive MPF complexes.

In the present study, we detected NS1 in the cytoplasm in the early stage postinfection (within 48 h) and in the nucleus at the late stage postinfection (96 h). This differential localization of NS1 after B19 virus infection may be reflected in NS1-associated functions, such as viral genome replication, gene expression, and induction of apoptosis and G_2 arrest. In fact, only the cells positive for NS1 in their cytoplasms showed the accumulation of cyclin B1 in the cytoplasms, suggesting a correlation between NS1 expression in the cytoplasm and cyclin B1 accumulation in the cyctoplasm. We are interested in the possibility that NS1 in the cytoplasm may be implicated in the accumulation of cyclin B1.

Human immunodeficiency virus type 1 (HIV-1) and human cytomegalovirus (HCMV) have been shown to induce the G_2 arrest of their infected cells. In HIV-1-infected cells, Vpr expression leads to inactivation of MPF caused by inactivation of cdc25 (23). The inactivation of cdc25 was recently revealed to be mediated by inhibition of nuclear import of serine/threonine protein phosphatase 2A (PP2A), known as an activator for cdc25, through a direct interaction between Vpr and PP2A (6). HCMV was found to alter expression levels of cyclins E, A, and B1 in the infected cells, resulting in both G_1 and G_2 arrests (7). In the case of B19 virus infection, however, the MPF was activated and mRNA levels of the cyclins were not increased. These data indicate that parvovirus B19 has a unique mechanism for regulation of the cell cycle.

B19 virus is known to be cytotoxic to erythroid target cells (9, 22, 26). In the B19 virus-infected UT7/Epo-S1 cells, apoptotic cells are readily detectable after 48 h of infection following the peak of G_2 arrest. The cell cycle control and its checkpoint

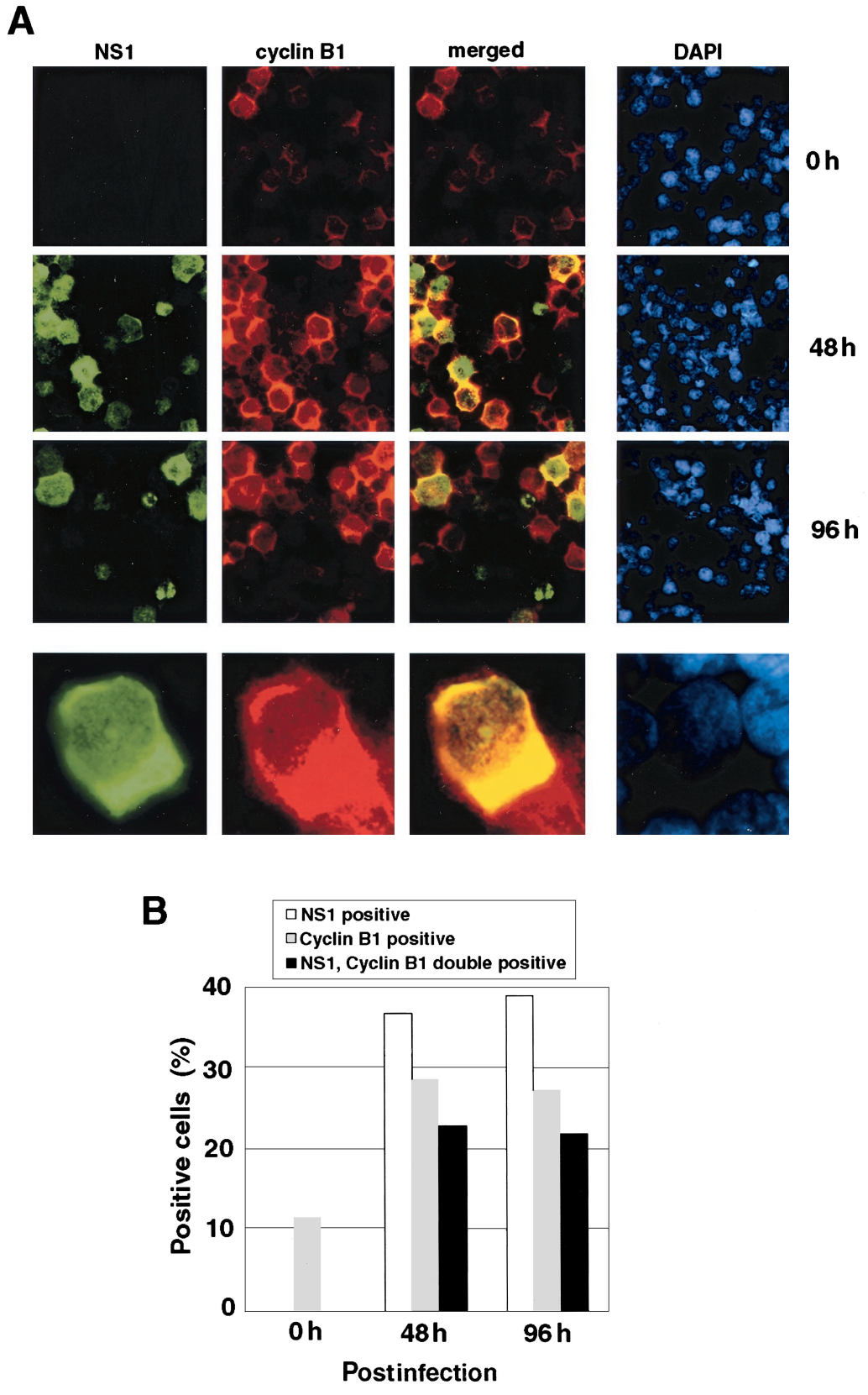

FIG. 6. Cytoplasmic accumulation of cyclin B1 in NS1-positive cells. (A) B19 virus-infected UT7/Epo-S1 cells were stained for NS1 (green), cyclin B1 (red), and DNA (blue) with anti-NS1 MAb, anti-cyclin B1 antibody, and 4′, 6′-diamidino-2-phenylindole (DAPI), respectively, 0, 48, and 96 h after infection. Magnified pictures are shown in the lower panels. The yellow color in the merged images represents colocalization of NS1 and cyclin B1. (B) Percentages of NS1-positive, cyclin B1-positive, and both NS1- and cyclin B1-positive cells in panel A were counted.

signaling are closely related to activation of the apoptosis-inducing pathway; p53 has been considered to be a regulator for either apoptosis induction or G_2 arrest (20). In this context, we reported that B19 virus-infected cells have apoptotic features in an NIHF tissue, in which expression of p53 and activated caspase-3 are increased (26). Furthermore, we detected enhanced phosphorylation of p53 in the B19 virus-infected UT7/Epo-S1 cells (data not shown). These data suggest that p53 plays an important role in B19 virus-induced apoptosis. Although NS1 is known to be involved in B19 virus-induced apoptosis, little is known about the molecular relationship between p53 and NS1, and further analyses will be required to understand the cell cycle regulation and apoptosis induction mediated by parvovirus B19.

ACKNOWLEDGMENTS

We thank L. C. Ndhlovu for critically reading the manuscript.

This work was supported in part by a grant for Core Research for Evolutional Science and Technology (CREST) of the Japan Science and Technology Corporation and Grant-in-Aid for Scientific Research A from the Ministry of Education, Science, Sports, and Culture of Japan.

REFERENCES

1. **Asao, H., Y. Sasaki, T. Arita, N. Tanaka, K. Endo, H. Kasai, T. Takeshita, Y. Endo, T. Fujita, and K. Sugamura.** 1997. Hrs is associated with STAM, a signal-transducing adaptor molecule. Its suppressive effect on cytokine-induced cell growth. J. Biol. Chem. **52:**32785–32791.
2. **Brown, K. E., and N. S. Young.** 1996. Parvoviruses and bone marrow failure. Stem Cells **14:**151–163.
3. **Darzynkiewicz, Z., S. Bruno, D. G. el Bino, W. Gorczyca, M. A. Hotz, P. Lassota, and F. Traganos.** 1992. Features of apoptotic cells measured by flow cytometry. Cytometry **13:**795–808.
4. **Gerace, L., and G. Blobel.** 1980. The nuclear envelope lamina is reversibly depolymerized during mitosis. Cell **19:**277–287.
5. **Guo, X. W., J. P. Th'ng, R. A. Swank, H. J. Anderson, C. Tudan, E. M. Bradbury, and M. Roberge.** 1995. Chromosome condensation induced by fostriecin does not require p34cdc2 kinase activity and histone H1 hyperphosphorylation, but is associated with enhanced histone H2A and H3 phosphorylation. EMBO J. **14:**976–985.
6. **Hrimech, M., X. J. Yao, P. E. Branton, and E. A. Cohen.** 2000. Human immunodeficiency virus type 1 Vpr-mediated G(2) cell cycle arrest: Vpr interferes with cell cycle signaling cascades by interacting with the B subunit of serine/threonine protein phosphatase 2A. EMBO J. **19:**3956–3967.
7. **Jault, F. M., J.-M. Jault, F. Ruchti, E. A. Fortunato, C. Clark, J. Corbeil, D. D. Richman, and D. H. Spector.** 1995. Cytomegalovirus infection induces high levels of cyclins, phosphorylated Rb, and p53, leading to cell cycle arrest. J. Virol. **69:**6697–6704.
8. **King, R. W., P. K. Jackson, and M. W. Kirschner.** 1994. Mitosis in transition. Cell **79:**563–571.
9. **Moffatt, S., N. Yaegashi, K. Tada, N. Tanaka, and K. Sugamura.** 1998. Human parvovirus B19 nonstructural (NS1) protein induces apoptosis in erythroid lineage cells. J. Virol. **72:**3018–3028.
10. **Morgan, D. O.** 1995. Principles of CDK regulation. Nature **374:**131–134.
11. **Ookata, K., S. Hisanaga, T. Okano, K. Tachibana, and T. Kishimoto.** 1992. Relocation and distinct subcellular localization of p34cdc2-cyclin B complex at meiosis reinitiation in starfish oocytes. EMBO J. **11:**1763–1772.
12. **Ozawa, K., G. Kurtzman, and N. Young.** 1986. Replication of the B19 parvovirus in human bone marrow cell cultures. Science **233:**883–886.
13. **Ozawa, K., G. Kurtzman, and N. Young.** 1987. Productive infection by B19 parvovirus of human erythroid bone marrow cells in vitro. Blood **70:**384–391.
14. **Ozawa, K., and N. Young.** 1987. Characterization of capsid and noncapsid proteins of B19 parvovirus propagated in human erythroid bone marrow cell cultures. J. Virol. **61:**2627–2630.
15. **Page, A. M., and P. Hieter.** 1999. The anaphase-promoting complex: new subunits and regulators. Annu. Rev. Biochem. **68:**583–609.
16. **Pines, J.** 1995. Cyclins and cyclin-dependent kinases: theme and variations. Adv. Cancer Res. **66:**181–212.
17. **Pines, J., and T. Hunter.** 1991. Human cyclins A and B1 are differentially located in the cell and undergo cell cycle-dependent nuclear transport. J. Cell Biol. **115:**1–17.
18. **Pines, J., and T. Hunter.** 1994. The differential localization of human cyclins A and B is due to a cytoplasmic retention signal in cyclin B. EMBO J. **13:**3772–3781.
19. **Reddy, G. P.** 1994. Cell cycle: regulatory events in G1→S transition of mammalian cells. J. Cell Biochem. **54:**379–386.
20. **Rich, T., R. L. Allen, and A. H. Wyllie.** 2000. Defying death after DNA damage. Nature **407:**777–783.
21. **Shimomura, S., N. Komatsu, N. Frickhofen, S. Anderson, S. Kajigaya, and N. S. Young.** 1992. First continuous propagation of B19 parvovirus in a cell line. Blood **79:**18–24.
22. **Sol, N., J. Le Junter., I. Vassias, J. M. Freyssinier, A. Thomas, A. F. Prigent, B. B. Rudkin, S. Fichelson, and F. Morinet.** 1999. Possible interactions between the NS-1 protein and tumor necrosis factor alpha pathways in erythroid cell apoptosis induced by human parvovirus B19. J. Virol. **73:**8762–8770.
23. **Stewart, S. A., B. Poon, J. B. Jowett, and I. S. Chen.** 1997. Human immunodeficiency virus type 1 Vpr induces apoptosis following cell cycle arrest. J. Virol. **71:**5579–5592.
24. **Tornusciolo, D. R., R. E. Schmidt, and K. A. Roth.** 1995. Simultaneous detection of TDT-mediated dUTP-biotin nick end-labeling (TUNEL)-positive cells and multiple immunohistochemical markers in single tissue sections. BioTechniques **19:**800–805.
25. **Toyoshima-Morimoto, F., E. Taniguchi, N. Shinya, A. Iwamatsu, and E. Nishida.** 2001. Polo-like kinase 1 phosphorylates cyclin B1 and targets it to the nucleus during prophase. Nature **410:**215–220.
26. **Yaegashi, N., T. Niinuma, H. Chisaka, S. Uehara, S. Moffatt, K. Tada, M. Iwabuchi, Y. Matsunaga, M. Nakayama, C. Yutani, Y. Osamura, E. Hirayama, K. Okamura, K. Sugamura, and A. Yajima.** 1999. Parvovirus B19 infection induces apoptosis of erythroid cells in vitro and in vivo. J. Infect. **39:**68–76.
27. **Yaegashi, N., T. Niinuma, H. Chisaka, T. Watanabe, S. Uehara, K. Okamura, S. Moffatt, K. Sugamura, and A. Yajima.** 1998. The incidence of, and factors leading to, parvovirus B19-related hydrops fetalis following maternal infection: report of 10 cases and meta-analysis. J. Infect. **37:**28–35.
28. **Yaegashi, N., K. Tada, H. Shiraishi, T. Ishii, K. Nagata, and K. Sugamura.** 1989. Characterization of monoclonal antibodies against human parvovirus B19. Microbiol. Immunol. **33:**561–567.
29. **Yang, J., E. S. Bardes, J. D. Moore, J. Brennan, M. A. Powers, and S. Kornbluth.** 1998. Control of cyclin B1 localization through regulated binding of the nuclear export factor CRM1. Genes Dev. **12:**2131–2143.
30. **Yang, J., H. Song, S. Walsh, E. S. Bardes, and S. Kornbluth.** 2001. Combinatorial control of cyclin B1 nuclear trafficking through phosphorylation at multiple sites. J. Biol. Chem. **276:**3604–3609.